THE ASTROPHYSICAL JOURNAL, 238:867–873, 1980 June 15

THE NGC 2264 MOLECULAR CLOUD: AMMONIA AND OH OBSERVATIONS

KENNETH R. LANG AND ROBERT F. WILLSON
Department of Physics, Tufts University
Received 1979 November 9: accepted 1979 December 17

ABSTRACT

Line emission from OH and NH_3 has been mapped in the region of the young star cluster NGC 2264. The NH_3 emission has been resolved into two components which are joined by a major axis lying along the galactic plane. A systematic velocity gradient of 3 km s^{-1} has been measured across the 2 pc extent of the NH_3 emission, and this gradient is interpreted in terms of a "rotation" of the two components about a minor axis centered midway between them and inclined at 90° to the galactic plane. The inferred rotation period of 4 million years corresponds to a Keplerian mass of $\sim 10^3\ M_\odot$. The NH_3 emission suggests an embryonic binary star system whose angular momentum could have been derived from the gravitational collapse of a differentially rotating interstellar cloud with a size of ~ 10 pc, a molecular hydrogen number density of ~ 5 cm^{-3}, a temperature of ~ 10 K, and a Jeans mass of $\sim 10^3\ M_\odot$. Because the OH emission is excited in the more tenuous parts of the region, it is more extensive and has a center shifted away from one of the NH_3 components in a direction where shearing motions may exist.

Subject headings: clusters: open — interstellar: molecules — nebulae: general — nebulae: individual — stars: formation

I. INTRODUCTION

The galactic cluster NGC 2264 has been thought to be a region of recent and continuing star formation ever since Herbig (1954) showed that this cluster contains T Tauri stars and Walker (1956) showed that many of the stars in this region lie above the main sequence in the Hertzsprung-Russell diagram. Observations of T Tauri stars and considerations of stellar evolution indicate that these stars are, in fact, relatively young, low-mass stars (ages on the order of 10^6 years and masses $\lesssim 2\ M_\odot$) which are approaching the main sequence along quasi-static equilibrium tracks (Rydgren, Strom, and Strom 1976). Because of their relatively young age, we might expect that the embryonic stars in NGC 2264 are still immersed within their placenta of gas and dust, and the individual stars within the cluster are thought to have the circumstellar dust shells which characterize recently formed stars (Strom, Strom, and Yost 1971). Moreover, the entire region shows diffuse Hα emission covered with wisps of dust, and the visible stars lie mainly in front of a large complex of gas and dust (Morgan *et al.* 1965).

Recent theoretical considerations suggest that star formation is extraordinarily inefficient, for the mass of the embryonic stars appears to be only a small fraction of that left behind in the dark dust clouds from which they formed (Larson 1969, 1973). Our observations of OH and ammonia, NH_3, in the direction of T Tauri stars in the Taurus-Auriga nebula and NGC 2264 indicate that small groups of T Tauri stars are, in fact, embedded within and kinematically associated with massive ($\gtrsim 100\ M_\odot$) molecular clouds with radii ~ 1 pc and kinetic temperatures ~ 20 K (Lang 1978; Lang and Willson 1979). The NGC 2264 molecular cloud was actually discovered after Allen (1972) found a strong infrared source [NGC 2264 (IR): $\alpha(1950.0) = 06^h38^m24^s.9$, $\delta(1950.0) = 09°32'29''$] which does not correspond with a visible star. Emission features of a host of molecules including CS, HCN, H_2S, SO, and NH_3 were soon detected in the direction of the IR source (Zuckerman *et al.* 1972; Thaddeus *et al.* 1972; Gottlieb and Ball 1973; and Mayer *et al.* 1973). The molecular emission in the direction of the IR source could have arisen from the circumstellar shell which surrounds the young star and gives rise to its infrared radiation, but Harvey, Campbell, and Hoffmann (1977) showed that the IR source is probably embedded within the more extensive dark cloud which lies mainly behind the visible stars in NGC 2264, and Rickard *et al.* (1977) showed that the 6 cm line emission of H_2CO in this direction is extended about 25′ north-south and 15′ east-west with a peak about 3′ north of the IR source. Moreover, the H_2CO line profiles suggested a very complicated velocity structure with three main components at LSR velocities of 5, 6.5, and 8 km s^{-1}, and velocity differences suggested rotation on an east-west axis. Nevertheless, their large half-power beamwidth of 6′.4 could not rule out the possibility that both the three-component velocity structure and the possible rotation are actually due to the superposition effects of different clouds within the antenna beam. Regardless of the apparently confusing nature of the kinematics of the NGC 2264 molecular cloud, it has been shown by Crutcher, Hartkopf, and Giguere (1978) and Lang and Willson (1979) that the main

molecular cloud which contains the IR protostar has a mass of a few thousand $M_\odot$, thereby confirming theoretical speculations that most of the mass of a molecular cloud is left behind during the process of star formation.

In this paper we present maps of the ammonia and OH emission in the direction of the main molecular cloud in NGC 2264 with high angular resolution (1.′4 beamwidth for NH_3 and 3.′4 beamwidth for OH). The most recent related work is that of Crutcher, Hartkopf, and Giguere (1978) who mapped the NGC 2264 region using the 2.6 mm lines of ^{12}CO and ^{13}CO with a half-power beamwidth of 2.′6. They found that the ^{13}CO emission coincides with the H_2CO cloud with the IR source located at one end of an elongated cloud centered about 4′ north of the IR source. The ^{13}CO cloud has an elongation of about 3:1 at a position angle of 150° east of north and a long axis which is parallel to the galactic plane. The ^{12}CO emission coincides with the ^{13}CO emission but also extends northward where additional clouds are found. The ^{12}CO velocity profiles suggest that there are multiple velocity components in most parts of the NGC 2264 region, but that the velocity of the main cloud changes significantly (~ 2 km s^{-1}) along its major axis. A detailed discussion of the kinematics of this ^{12}CO cloud was not possible, however, because of the possibility of multiple velocity components and also because of the unusual broadening of the ^{12}CO line from 2 km s^{-1} in the outer regions to 5.5 km s^{-1} in the central regions. In sharp contrast to the ^{12}CO profiles, our NH_3 profiles exhibit only one velocity component at each position and the line width remains at ~ 2 km s^{-1} at all regions within the main molecular cloud. When combined with our high angular resolution of 1.′4, this has enabled us to resolve the elongated cloud into two main components, and to delineate a systematic velocity gradient along the cloud's main axis. Although the NH_3 emission is confined to the region of the ^{13}CO emission and does not extend northward into the other ^{12}CO sources, the OH emission is peaked about 2′ north of the main NH_3 cloud and opens northward to the region of the ^{12}CO clouds. These differences reflect the fact that both ^{13}CO and NH_3 are excited in the dense regions of a molecular cloud, whereas both ^{12}CO and OH can be excited in the more tenuous regions.

II. OBSERVATIONS OF AMMONIA (NH_3) AND OH LINE EMISSION IN THE DIRECTION OF NGC 2264

The NH_3 observations were performed using the 36.6 m parabolic reflector at the Haystack Observatory. A horizontally polarized feed was employed which had a half-power beamwidth of 1.′4 and provided a peak sensitivity of 0.08 K = 1 Jy at 23,694.5 MHz, where the system noise temperature was ~ 150 K and the receiver noise temperature was ~ 60 K. A 1024 channel autocorrelator was employed with a total bandwidth of 6.67 MHz and a velocity resolution of 0.08 km s^{-1}. The receiver passband was centered at the rest frequency of the $(J, K) = (1, 1) = 23{,}694.495$ MHz rotation inversion transition of the NH_3 molecule. The data were then taken in the total power mode with position switching to a point 2.°5 or 10^m away in right ascension every 10 minutes of time. Temperature calibrations were made by using a noise tube. Our preliminary results (Lang and Willson 1979) indicated that spectra obtained after a few hours of integration show the splitting of the (1, 1) rotational inversion caused by quadrupole interaction, and that the ammonia emission peaks at the infrared source (IR) and another point P about 4′ away. Both peaks were of roughly equal intensity, but there seemed to be weaker emission between them. As discussed in the previous section, the IR source is a strong infrared point source which may be a protostar or a newly formed star.

We have now built upon our preliminary results and mapped the (1, 1) rotation inversion transition of NH_3 throughout most of the NGC 2264 region with a grid spacing of 1.′5. At each position the main component of the transition was fitted to a Gaussian line profile, and its peak antenna temperature T_A, its LSR velocity V_{LSR}, and its full width to half-maximum ΔV, were determined by the method of least squares. The results are given in Table 1, where the values of T_A have been corrected for the changing antenna sensitivity as a function of zenith angle, and the ΔV have been

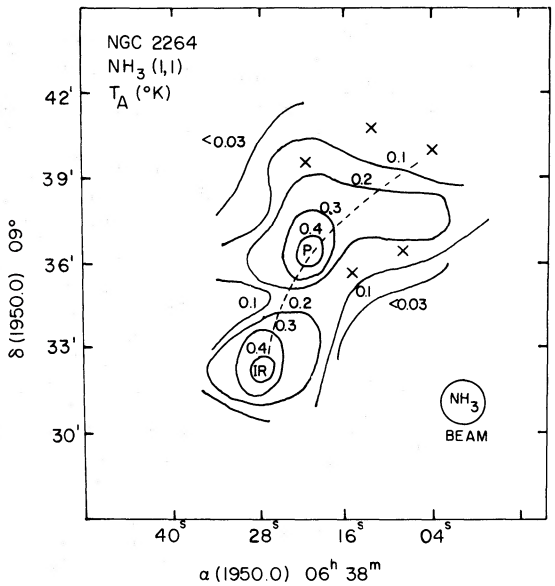

FIG. 1.—Contour maps of the antenna temperature of the $(J, K) = (1, 1)$ transition of the ammonia molecule at 23.695 GHz in the direction of the main molecular cloud in NGC 2264. The contour levels are at 0.4, 0.3, 0.2, and 0.1 K, the ammonia cloud contains two main components located at P and IR (an infrared protostar) separated by $\sim 4' \sim 0.9$ pc, and the region includes five T Tauri stars marked by crosses (V360 Mon, LU Mon, LT Mon, V419 Mon, and IP Mon; see Lang and Willson 1979). The dashed line denotes the axis along which velocity measurements have been taken (cf. Figs. 4 and 5). The cloud is elongated along a position angle of 150° which lies parallel to the galactic plane.

TABLE 1

PARAMETERS OF THE $(J, K) = (1, 1)$ ROTATION INVERSION TRANSITION OF THE NH_3 MOLECULE AT DIFFERENT POSITIONS IN THE YOUNG STAR CLUSTER NGC 2264

α(1950.0) and δ(1950.0)	T Tauri Star	T_A (K)	V_{LSR} (km s^{-1})	ΔV (km s^{-1})
$06^h37^m54^s$ 09°38′02″	NW Mon	<0.02	...	...
06 37 57 09 37 55	...	0.14 ± 0.02	5.70 ± 0.10	1.21 ± 0.25
06 38 03 09 37 55	...	0.23 ± 0.02	4.90 ± 0.07	1.23 ± 0.16
06 38 04 09 39 50	LT Mon	0.09 ± 0.007	5.30 ± 0.05	1.40 ± 0.12
06 38 08 09 33 26	...	<0.05	...	...
06 38 08 09 36 26	V419 Mon	0.14 ± 0.005	5.20 ± 0.05	1.80 ± 0.15
06 38 09 09 37 55	...	0.24 ± 0.01	5.40 ± 0.05	2.00 ± 0.13
06 38 09 10 29 40	...	<0.03	...	...
06 38 12 09 33 49	IO Mon	<0.02	...	...
06 38 12 09 40 49	LU Mon	<0.02	...	...
06 38 15 09 35 37	IP Mon	0.10 ± 0.003	6.00 ± 0.03	2.00 ± 0.06
06 38 15 09 36 25	...	0.11 ± 0.01	5.80 ± 0.09	2.50 ± 0.20
06 38 15 09 37 55	...	0.24 ± 0.02	5.50 ± 0.08	2.60 ± 0.20
06 38 16 09 32 00	...	<0.10	...	...
06 38 21 09 30 25	...	0.19 ± 0.03	7.50 ± 0.07	1.40 ± 0.15
06 38 21 09 34 55	...	0.16 ± 0.01	6.20 ± 0.07	1.75 ± 0.16
06 38 21 09 36 25	(P)	0.45 ± 0.009	6.00 ± 0.04	2.00 ± 0.10
06 38 21 09 37 55	...	0.30 ± 0.01	5.50 ± 0.04	3.00 ± 0.09
06 38 21 09 38 40	...	0.27 ± 0.06	5.58 ± 0.11	1.11 ± 0.27
06 38 21 09 39 25	V360 Mon	0.13 ± 0.05	5.50 ± 0.07	1.80 ± 0.20
06 38 21 09 42 25	...	<0.03	...	...
06 38 22 09 30 30	...	0.19 ± 0.02	7.84 ± 0.04	0.78 ± 0.10
06 38 22 09 32 00	...	0.19 ± 0.01	7.40 ± 0.05	2.40 ± 0.13
06 38 24 09 33 30	...	0.19 ± 0.01	7.30 ± 0.08	2.50 ± 0.20
06 38 25 09 29 30	V363 Mon	<0.02	...	...
06 38 27 09 33 00	(IR)	0.43 ± 0.008	7.50 ± 0.02	2.50 ± 0.05
06 38 27 09 34 55	...	<0.08	...	...
06 38 27 09 36 25	...	0.25 ± 0.01	5.60 ± 0.10	2.40 ± 0.08
06 38 27 09 37 55	...	<0.07	...	...
06 38 28 09 30 30	...	0.10 ± 0.01	8.30 ± 0.20	3.50 ± 0.50
06 38 28 09 31 30	...	0.37 ± 0.02	7.80 ± 0.07	2.60 ± 0.16
06 38 28 09 33 00	...	0.30 ± 0.01	6.90 ± 0.03	2.20 ± 0.09
06 38 28 09 34 30	...	0.09 ± 0.01	6.50 ± 0.20	3.70 ± 0.40
06 38 33 09 33 25	...	<0.05	...	...
06 38 33 09 36 25	...	0.10 ± 0.01	5.70 ± 0.10	3.30 ± 0.25
06 38 34 09 30 30	...	<0.05	...	...
06 38 34 09 32 00	...	0.24 ± 0.01	6.20 ± 0.05	2.10 ± 0.12

corrected for instrumental broadening. Corrections for atmospheric opacity at 23 GHz were not included because they are smaller than the measurement uncertainties. The measurement errors given in Table 1 are the formal errors in the Gaussian fit at the 1 σ level.

The data given in Table 1 were used to make the contour map of antenna temperature displayed in Figure 1. The overall shape of the distribution of the NH_3 antenna temperature is similar to that of the distribution of the ^{13}CO antenna temperature given by Crutcher, Hartkopf, and Giguere (1978). Both distributions are elongated along the galactic plane at a position angle of ~150° east of north, and both distributions exhibit an extension to the west. In both cases the elongated cloud has an extent of ~15′ along the main axis with an elongation of about 3:1. Our narrower antenna beamwidth, however, has allowed us to show that the elongated molecular cloud has fragmented into two components, one centered on the infrared protostar, IR, and the other at a point *P* about 4′ or 0.9 pc northwest of the protostar. Thus the main molecular cloud appears to be an embryonic binary star system. Each of the "protostar" components is about 4′ or 0.9 pc in size (assuming a distance of 760 pc as given by Raimond 1966). In addition to these two major features, a weaker "arm" extends about 3′ to the west in the direction of the T Tauri stars V419 Mon and IP Mon. We were unable to detect any NH_3 emission with an antenna temperature greater than 0.02 K in the direction of the northern components detected by Crutcher, Hartkopf, and Giguere with the ^{12}CO emission line, but this is not surprising for they also failed to detect these components with the ^{13}CO emission line. Both the ^{13}CO and NH_3 lines are excited in the dense regions illustrated in Figure 1, and it is these regions which contain most of the mass. The additional northern components seen with the ^{12}CO emission line are probably very tenuous regions containing less mass.

We also observed the same region at the 1667.359 MHz transition of the OH molecule using the 305 m spherical reflector of the Arecibo Observatory. A circularly polarized line feed was employed which had a half-power beamwidth of 3′.4 and provided a peak

sensitivity of 6.2 K = 1 Jy at 1667 MHz. The left-hand circularly polarized antenna signal was connected to a system whose receiver temperature was ~100 K, and the intermediate-frequency signal was divided into two 20 MHz passbands centered at the $F = 1$–1 and the $F = 2$–2 hyperfine split, lambda doublet transitions of the $^2\Pi_{3/2}$, $J = 3/2$ ground state of the OH molecule (at 1665.402 and 1667.359 MHz, respectively). A 252 channel autocorrelator with a bandwidth of 1.25 MHz was used to provide spectra with a velocity resolution of 0.9 km s^{-1}. In order to minimize instrumental conditions which might produce spurious spectra, frequency switching at ±0.625 MHz was used, and the difference spectra were subsequently folded and added to give spectra which were corrected to the local standard of rest. At each position the intensities of the 1667 and 1665 MHz lines were consistent with the LTE ratio of 9 to 5, and the stronger 1667 MHz line was fitted to a Gaussian line profile to give the line parameters shown in Table 2.

The data given in Table 2 were used to make the contour map of antenna temperature displayed in Figure 2. Although the OH emission is elongated in the same direction as the NH_3 emission, the OH peak is shifted about 2′ west of component *P* of the NH_3 map and there is relatively weak OH emission at the infrared source IR. Moreover, the OH emission opens up and extends northward in a way which suggests that its excitation conditions are similar to those of ^{12}CO. In fact, we attribute the differences between the NH_3 and OH maps to the different excitation conditions of the two molecules, for OH can be excited in the more tenuous regions where the molecular hydrogen density is low ($n_{H_2} \sim 50$–100 cm^{-3}), whereas the ammonia emission requires dense regions with $n_{H_2} > 4000$ cm^{-3}. This difference in excitation is also responsible for the difference between the ^{12}CO and the ^{13}CO map given by Crutcher, Hartkopf, and Giguere (1978).

Of special interest is the fact that the main line of the NH_3 rotation inversion transition consisted of only one component at each position whose central velocity varied systematically with position but whose half-width remained essentially unchanged. As illustrated in Figure 3 and Table 1, the main line of the two components at IR and *P* have respective half-widths of 2.5 ± 0.05 and 2.00 ± 0.10 km s^{-1} with a velocity difference of 1.5 ± 0.03 km s^{-1}. These results may be compared with those of Rickard *et al.* (1977) which suggested that the H_2CO line profiles are the convolution of three velocity components of 5, 6.5, and 8 km s^{-1}, and also with the results of Crutcher, Hartkopf, and Giguere (1978), which showed that the ^{12}CO line has a half-width of 5.5 km s^{-1} at IR and *P*. Our results suggest that there are no multiple velocity components within the main molecular cloud of NGC 2264, and that the H_2CO results are the consequence of using a large antenna beamwidth of 6′.5 which covered a region containing a systematic velocity gradient as well as two intense components with different velocities. The broadening of the ^{12}CO line at a position of maximum line strength has often been interpreted in terms of the radial collapse of a molecular cloud, but Crutcher *et al.* concluded that sorting out any collapse of the NGC 2264 molecular cloud in the presence of several velocity components would require higher spatial and velocity resolution. Although there is a remote possibility that the outer surface layers detected by the ^{12}CO line emission may be undergoing collapse, we find no evidence for collapse in either the central velocities or the line widths of either our NH_3 or our OH emission lines. Instead, the two high-density cores measured by the NH_3 lines may each be in hydrostatic equilibrium while rotating in Keplerian orbits about a common center of mass.

TABLE 2

PARAMETERS OF THE 1667 MEGAHERTZ TRANSITION OBSERVED IN THE DIRECTION OF THE NGC 2264 MOLECULAR CLOUD

α(1950.0) and δ(1950.0)	T_A (K)	V_{LSR} (km s^{-1})	ΔV (km s^{-1})
06^{h}37^{m}58^s 09°34′30″	0.54	5.6	1.7
06 37 58 09 37 30	0.57	5.5	2.4
06 37 58 09 39 00	0.58	5.7	2.2
06 37 58 09 40 30	0.44	5.9	1.9
06 38 10 09 34 30	0.37	5.6	3.1
06 38 10 09 37 30	0.87	5.7	1.7
06 38 10 09 39 00	0.83	5.6	2.4
06 38 10 09 42 00	0.48	5.5	2.6
06 38 22 09 28 30	<0.2	...	...
06 38 22 09 33 00	0.49	6.3	3.1
06 38 22 09 34 30	0.54	6.3	3.4
06 38 22 09 37 30	0.63	5.4	3.0
06 38 22 09 39 00	0.62	5.6	2.6
06 38 22 09 42 00	0.38	5.6	3.0
06 38 28 09 31 30	0.27	7.0	4.5
06 38 28 09 34 30	0.52	6.4	2.3
06 38 28 09 36 00	0.49	5.9	2.4
06 38 28 09 37 30	0.40	5.6	3.1
06 38 28 09 39 00	0.68	5.5	2.0
06 38 28 09 40 30	0.57	5.4	1.8
06 38 34 09 30 00	0.30	5.8	4.1
06 38 34 09 33 00	0.40	5.7	2.9
06 38 34 09 34 30	0.39	5.7	3.6
06 38 34 09 36 00	0.39	5.7	2.3
06 38 34 09 37 30	0.32	5.1	2.3
06 38 34 09 40 30	0.42	5.3	1.3

NOTE.—Typical measurement uncertainties at the standard deviation are ±0.05 K in antenna temperature and ±0.2 km s^{-1} in velocity.

III. DISCUSSION

We have shown that the main molecular cloud in NGC 2264 is composed of two components, each about 0.9 pc in total extent and separated by about 0.9 pc. Taking the dominant excitation mechanism for the ammonia lines to be due to collisions with molecular hydrogen, each component must have a total mass of $M \gtrsim 100\ M_\odot$. Masses of this order have a gravitational potential energy which is comparable to their thermal energy for the assumed radii and the measured kinetic temperatures of ~20 K (Lang 1978). Crutcher, Hartkopf, and Giguere (1978) use CO

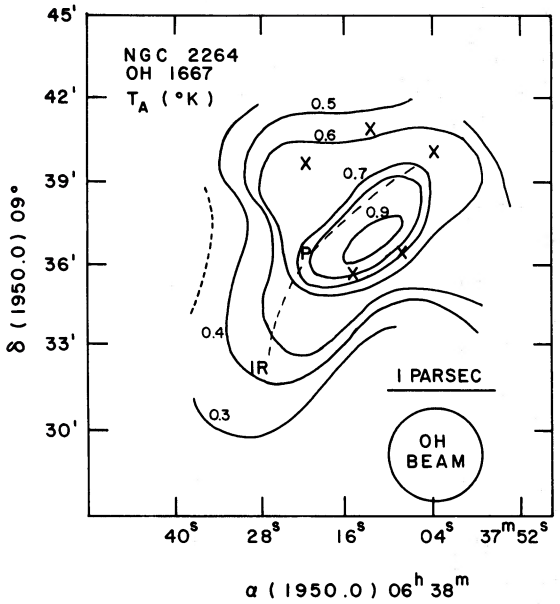

FIG. 2.—Contour maps of the antenna temperature of the $F = 1$–1 transition of the OH molecule at 1667 MHz in the direction of the main molecular cloud in NGC 2264. The contour levels are at 1.0, 0.9, 0.8, 0.7, 0.6, 0.5, and 0.4 K. The OH cloud is centered 2′ to the west of the peak of the northern component of the NH_3 cloud, and it exhibits only weak emission at the infrared (IR) source. The region includes five T Tauri stars marked by crosses, and the dashed line denotes the axis along which NH_3 velocities have been taken (cf. Figs. 4 and 5). The cloud is elongated along a position angle of 150° which lies parallel to the galactic plane.

column densities to derive masses on the order of $10^3\ M_\odot$ for different locations within the main molecular cloud. We will adopt $M = 500\ M_\odot$ as the mass of each component because there is no evidence for collapse, hydrostatic equilibrium appears likely, and these masses are within an order of magnitude of the CO results.

As illustrated in Figure 5, the NH_3 velocities that fall along the dashed line drawn perpendicular to the contours of equal velocity (Fig. 4) show a systematic velocity gradient of 3 km s^{-1} over the 2 pc extent of the cloud. The apparent radial velocity caused by galactic rotation is $\sim$7 km s^{-1} at the position and distance of NGC 2264, and this means that we can interpret Figure 5 in terms of a "rotation" at 1.5 km s^{-1} about a minor axis that lies 60° east of north and is centered midway between the two condensations where the $V_{LSR} \sim 6.5$ km s^{-1} is due to galactic rotation. Assuming a velocity difference of 1.5 km s^{-1} between the center of "rotation" and the outer edges of the system located at a radius of $\sim$1 pc, we obtain an angular rotation velocity of 1.5×10^{-6} rad yr^{-1} and a "rotation" period of 4×10^6 years, assuming that the rotation axis is perpendicular to the line of sight. Rotation periods of 5 million years were previously inferred by Rickard *et al.* (1977) for east-west rotation and by Crutcher, Hartkopf, and Giguere (1978) for rotation about an axis perpendicular to the direction of cloud elongation. Because the time to complete one rotation is only a factor of 10 larger than the free-fall time for each component, and also because the "rotation" time is comparable to the ages of the T Tauri stars found in this region, we use the word "rotation" with caution and take it to suggest future rotation of the gravitationally bound components about a common center of mass.

The radial velocity data for the southern part of the NH_3 cloud ($V_{LSR} > 6.3$ km s^{-1} and distance < 0.5 pc in Fig. 5) are consistent with solid-body rotation in which the observed radial velocities are interpreted in terms of a linear increase in rotational velocity with increasing distance from the cloud center. The more gradual decrease in radial velocity in the northwest part of the NH_3 cloud ($V_{LSR} < 6.3$ km s^{-1} and distance > 0.5 pc in Fig. 5) suggests that projection effects

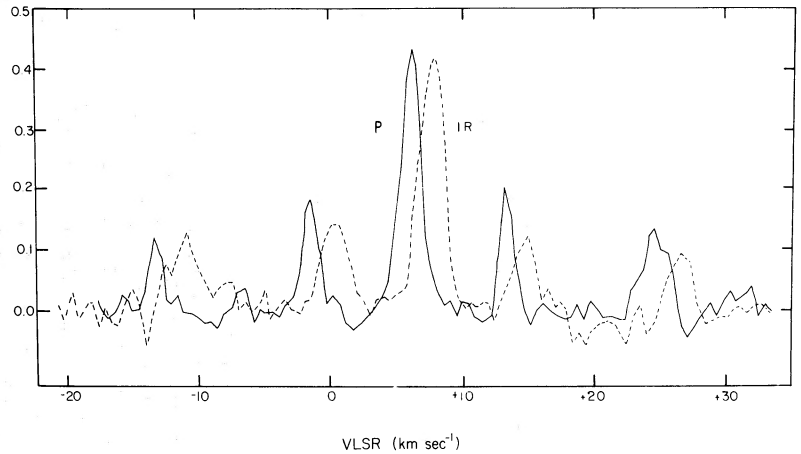

FIG. 3.—The $(J, K) = (1, 1)$ rotation inversion transitions of the ammonia molecule observed in emission in the direction of the two most intense components (IR and P) of the main molecular cloud in NGC 2264. The point $V_{LSR} = 0$ corresponds to the main component of the (1, 1) transition at 23,694.495 MHz. The (1, 1) rotational inversion is split by quadrupole interaction to give the four satellite lines, and the velocity scale corresponds to the velocity with respect to the local standard of rest (V_{LSR}) for the more intense main line. Note that there are no multiple velocity components, that the lines are narrow ($\sim$2 km s^{-1}), and that the two components are separated by $\sim$1.5 km s^{-1}.

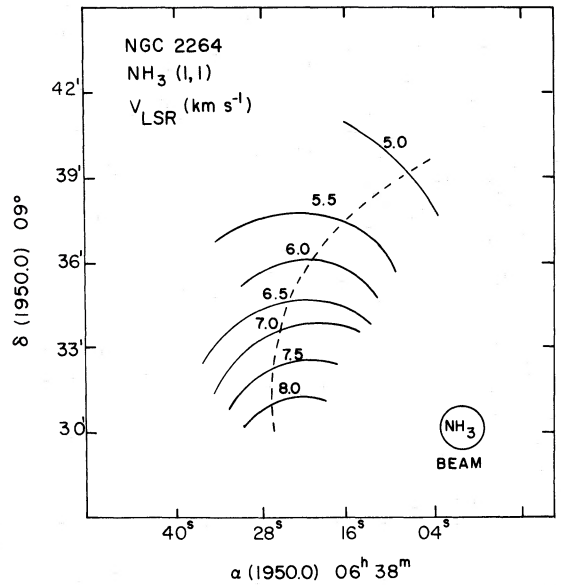

FIG. 4.—Contour maps of the velocity with respect to the local standard of rest, V_{LSR}, of the $(J, K) = (1, 1)$ transition of the ammonia molecule at 23.695 GHz in the direction of the main molecular cloud in NGC 2264. The contour levels are 8.0, 7.5, 7.0, 6.5, 6.0, 5.5, and 5.0 km s^{-1}. The dashed line denotes the axis along which the velocities shown in Figure 5 lie, and it is roughly parallel to the galactic plane.

or nonrotational shearing motions are distorting solid-body rotation in this direction. In fact, the distributions of both OH and NH_3 (Figs. 1 and 2) suggest that there may have been some nonrotational motions away from component P in the northwest direction.

At any rate, the mass given by Kepler's third law for a rotation period of 4 million years and a component separation of 1 pc is $\sim 10^3\ M_\odot$, suggesting that the components P and IR may be in gravitational equilibrium while rotating about a common center of mass. Although the observed "rotational" velocities are a factor of 100 times too large to be due to differential galactic rotation across the molecular cloud, the observed angular momentum could have been derived from the differential galactic rotation of an interstellar cloud of about 10 pc in diameter which underwent gravitational collapse to form the currently observed molecular cloud. In this case the interstellar cloud might have had a molecular hydrogen density of $\sim 5\ \mathrm{cm}^{-3}$, which is typical of diffuse interstellar clouds, and at a temperature of ~ 10 K the Jeans mass required for gravitational collapse would have been $\sim 10^3\ M_\odot$, which is the approximate mass of the molecular cloud.

Radio astronomy at the Haystack Observatory of the Northeast Radio Observatory Corporation is supported by the National Science Foundation. The Arecibo Observatory is part of the National Astronomy and Ionospheric Center, which is operated by Cornell University under contract with the National Science Foundation. Part of this work was done while one of us (R. F. W.) was finishing his Ph.D. thesis under a fellowship from the Arecibo Observatory. We thank the Tufts University Computer Staff for computing assistance while doing this research. This research was partially supported by a grant from the American Astronomical Society.

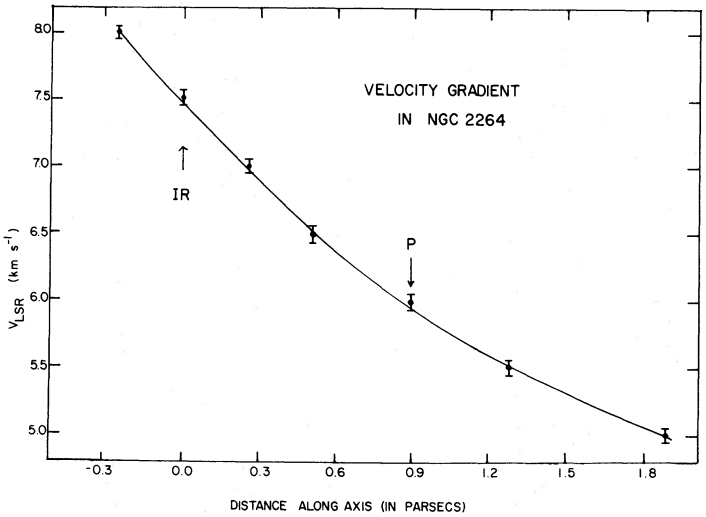

FIG. 5.—Velocity measurements along the main axis of the main molecular cloud in NGC 2264 (axis denoted by a dashed line in Figs. 1, 2, and 4). Here the points correspond to the velocity with respect to the local standard of rest, V_{LSR}, of the $(J, K) = (1, 1)$ transition of the ammonia molecule at 23.695 GHz, and the error bars denote the measurement uncertainties at the one standard deviation level. The ammonia cloud contains two main components located at P and IR (an infrared protostar) separated by 0.9 pc (assumed distance 760 pc). The figure illustrates a systematic velocity gradient of ~ 3 km s^{-1} over the 2 pc extent of the main molecular cloud.

REFERENCES

Allen, D. A. 1972, *Ap. J.* (*Letters*), **172**, L55.
Crutcher, R. M., Hartkopf, W. I., and Giguere, P. I. 1978, *Ap. J.*, **226**, 839.
Gottlieb, C. A., and Ball, J. A. 1973, *Ap. J.* (*Letters*), **184**, L59.
Harvey, P. M., Campbell, M. F., and Hoffmann, W. F. 1977, *Ap. J.*, **215**, 151.
Herbig, G. H. 1954, *Ap. J.*, **119**, 483.
Lang, K. R. 1978, *Moon and Planets*, **19**, 185.
Lang, K. R., and Willson, R. F. 1979, *Ap. J.*, **227**, 163.
Larson, R. B. 1969, *M.N.R.A.S.*, **145**, 271.
———. 1973, *Ann. Rev. Astr. Ap.*, **11**, 219.
Mayer, C. H., Waak, J. A., Cheung, A. C., and Chiu, M. F. 1973, *Ap. J.* (*Letters*), **182**, L65.
Morgan, W. W., Hiltner, W. A., Neff, J. S., Garrison, R., and Osterbrock, D. E. 1965, *Ap. J.*, **142**, 974.
Raimond, E. 1966, *Bull. Astr. Inst. Netherlands*, **18**, 191.
Rickard, L. J., Palmer, P., Buhl, D., and Zuckerman, B. 1977, *Ap. J.*, **213**, 654.
Rydgren, A. E., Strom, S. E., and Strom, K. M. 1976, *Ap. J. Suppl.*, **30**, 307.
Strom, K. M., Strom, S. E., and Yost, J. 1971, *Ap. J.*, **165**, 479.
Thaddeus, P., Kutner, M. L., Penzias, A. A., Wilson, R. W., and Jefferts, K. B. 1972, *Ap. J.* (*Letters*), **176**, L73.
Walker, M. F. 1956, *Ap. J. Suppl.*, **2**, 365.
Zuckerman, B., Morris, M., Palmer, P., and Turner, B. E. 1972, *Ap. J.* (*Letters*), **173**, L125.

KENNETH R. LANG and ROBERT F. WILLSON: Department of Physics, Tufts University, Medford, MA 02155